

Dominant effect of support wettability on the reaction pathway for *Catalytic Wet Air Oxidation* over Pt and Ru nano-particle catalysts

Dafydd Davies^a, Stanislaw Golunski^{a*}, Peter Johnston^b, Georgi Lalev^a and Stuart Taylor^a

^a Cardiff Catalysis Institute, School of Chemistry, Cardiff University, Cardiff CF10 3AT, UK

^b Johnson Matthey Plc, Orchard Road, Royston SG8 5HE, UK

*Correspondence to Stanislaw Golunski

Tel: +44-292-0870826 email: GolunskiSE@cardiff.ac.uk

Abstract

Support wettability can play a key role in directing the activation of oxygen during *catalytic wet air oxidation* over nano-particle catalysts. When the nano-particles are comprised of metallic Pt, the optimum support is hydrophobic, but when they are ionic Ru, a hydrophilic support is more effective. This reversal in support effect is consistent with two distinct surface pathways: one in which gas-phase O₂ is directly adsorbed on the Pt⁰ surface; the other in which dissolved O₂ is activated on RuO₂ immersed in the contaminated aqueous phase. The known effects of ceria on these precious metal catalysts are of secondary importance to support wettability.

Key words: CWAO, platinum, ruthenium, ceria, hydrophobicity, hydrophilicity, phenol

Wet air oxidation, which was patented and first commercialised in the 1950s¹, is a technique for purifying wastewater by converting organic contaminants to CO₂ and H₂O using air as the oxidant. Although it has the environmental and economic benefits of avoiding the use of hazardous oxidising agents (such as chlorine, ozone or hydrogen peroxide), it has the drawbacks of being an energy intensive process with a high capital cost. These drawbacks arise mainly from the need to operate the process at high pressures (eg 30 bar for phenol removal²) in order to keep the water in the liquid phase at the temperatures required to achieve an acceptable rate of deep oxidation of the organic contaminants.³

The use of catalysis in wet air oxidation offers the prospect of operating at lower temperatures, which in turn would reduce the pressure required to maintain the water in the liquid phase. However, there is a potential trade-off, as the solubility of O₂ in water decreases with decreasing temperature over the temperature and pressure ranges currently required for *catalytic wet air oxidation* (CWAO), limiting the mass transfer of oxygen from the gas phase to the liquid phase.⁴ The longstanding aim in the field of CWAO, therefore, has been to operate the process at normal pressure, and at temperatures below 100 °C where oxygen solubility increases with decreasing temperature⁵. To date, the lowest operating temperatures are typically between 150 and 200 °C,⁶ and therefore require pressures between 4 and 15 bar_g.

Numerous homogeneous and heterogeneous catalyst formulations are known to be active for CWAO, including functionalised carbons⁷, pillared clays⁸ and graphene oxide⁹, in addition to more conventional metal-oxide and supported-metal oxidation catalysts¹⁰. Among the most active and stable catalysts are those based on platinum and ruthenium,^{11,12} especially when supported on ceria¹³ or ceria-titania^{14,15}. Here we report that the apparent rate of CWAO of phenol over these precious metals, measured during continuous testing in a trickle-bed reactor, shows a specific dependence on the wettability of the support material, which allows the operating temperature to be decreased below 150 °C. In our tests, we have excluded the effects arising from changes in viscosity, oxygen solubility and external mass transfer, by comparing the CWAO activity of different Pt and Ru formulations under self-consistent operating conditions.

Our benchmark catalyst (Pt/Al₂O₃) was comprised of 2% by mass of platinum dispersed on granular alumina (γ -Al₂O₃ with 0.425 - 0.6 mm grain size), which had been prepared from a chloride-free platinum precursor using a conventional dry impregnation route (see SI – Catalyst Preparation). It had a Brunauer-Emmett-Teller (BET) surface area of 97 m² g⁻¹, with most of its internal volume arising from a very narrow pore-size distribution (2-4 nm at mid height).

Transmission electron microscopy (TEM) showed that the platinum was in the form of regularly shaped nano-particles with a mean diameter of 8.1 nm, while a combination of X-ray diffraction (XRD) and temperature-programmed reduction (TPR) indicated that it was predominantly, but not exclusively, in the metallic form (see SI – Catalyst Characterisation).

Whereas the classic methods for studying the wettability of solid materials rely on macroscopic measurements of contact angles,¹⁶ we have been developing a technique which uses cryo-electron tomography (CET) to examine the local interactions of our catalysts with liquid water over a much shorter length scale (currently comparable to the grain size of the catalyst). CET, which is often used in cellular biology¹⁷, allows magnified 3-D reconstructions to be created from multiple 2-D TEM images taken from a range of different angles. In our studies, the catalyst sample was sprayed with a fine mist of water, before the sample was rapidly cooled in liquid nitrogen. The effect was to vitrify the water in the shape it formed when the mist came into contact with the catalyst surface, without forming macroscopic ice crystals. In the case of the benchmark Pt/Al₂O₃, most of the vitrified water was visible as a thick layer around the catalyst grains (Figure 1a), together with some droplets that were attached to the catalyst surface with contact angles of around 90°. These observations are consistent with a largely electrophilic surface, as expected of high surface area alumina with well dispersed hydroxyl functionality that leads to H₂O molecules becoming attached over the entire surface through dipole interactions.¹⁸ When tested at 140 °C under our standard trickle-bed operating conditions (see SI – Catalyst Testing), this catalyst showed stable phenol conversion of 50 ±3% over a period of 4 hours (Figure 1b).

Using a methodology reported for the hydrophobation of γ -Al₂O₃ membranes,¹⁹ surface-modified variants of the Pt/Al₂O₃ catalyst were prepared, in which the alumina support material was silanated by immersion in dichlorophenylsilane solution (for either 1.5 or 5 h) prior to impregnation with the platinum precursor. The textural properties (BET surface area, pore volume, pore size distribution) of the resultant silanated catalysts were very similar to those of the unmodified Pt/Al₂O₃ (see SI – Catalyst Characterisation). However, when tested at 140 °C, the initial activity of the silanated catalysts was much higher, resulting in 80-90% phenol conversion (depending on the duration of the immersion step) over the first 2 hours (Figure 1b). CET confirmed that silanation had markedly changed the wettability of the surface. Instead of a continuous layer of vitrified water, large isolated spherical droplets with contact angles >90° were now visible, indicating that the silanated catalyst granules were distinctly

hydrophobic in nature. As Figure 1 b shows, though, the catalysts progressively desilanated during use, which resulted in their continuous deactivation over the 5 hours of testing.

The activity of Pt/Al₂O₃ could also be improved by additional calcination in flowing N₂ (Figure 1). When this was included as the final step in the preparation of the silanated catalyst, stable 90% phenol conversion could be achieved even at a temperature of 120 °C during 5 hours of testing (Figure 1c). Whereas textural and structural characterisation did not reveal any discernible changes after the additional calcination step, TPR showed a substantial attenuation in the size of the peak associated with the reduction of unstabilised residual Pt oxide on the surface of the metal nanoparticles, together with an increase in the size of the peak associated with more stable Pt oxide at the support interface (see SI – Catalyst Characterisation). We attribute the high activity achieved after silanation and N₂-calcination of Pt/Al₂O₃ to (i) the nature of the support being transformed from hydrophilic to hydrophobic around the nanoparticles, and (ii) an increased proportion of exposed metallic platinum in the nanoparticles. It is also worth noting that the increase in Pt oxide at the support interface appears to act as a diagnostic for improved stability of the silanated surface.

When the platinum was supported on granular β-SiC with a comparable grain size to the alumina, the resultant catalyst (Pt/SiC) had a lower BET surface area (22 m² g⁻¹) than the Pt/Al₂O₃, but it had a similar Pt particle size (7.7 nm). The Pt/SiC catalyst was both highly active and very durable for CWAO, achieving 99.95% conversion at 160 °C, which it maintained during repeated 6-hour tests over a period of several months. Significantly, the outlet concentration of phenol was consistently below our target value of 6.2 ppm by mass, which is the US Environmental Protection Agency safe limit for phenol discharged in wastewater.²⁰ The selectivity to CO₂ was consistently >95%, with the only by-products detected being the carboxylic acids (formic, acetic, fumaric, maleic) and the aromatic oxygenates (hydroquinone, benzoquinone, catechol, hydroxybenzoic acid) that lie on the reaction pathway proposed by Martín-Hernández *et al*²¹. Lowering the temperature to 120 °C reduced the phenol conversion by only 10%, so that it stabilised at around 90%.

Previous studies of passively oxidised silicon carbide (i.e. in the same condition as the support in our calcined Pt/SiC catalyst) have indicated that >70% of the surface has zero charge and therefore exhibits hydrophobic character, while the remainder is made up of negatively-charged hydrophilic regions where oxidation of the SiC has occurred.²² The CET images of our catalyst (Figure 2a) revealed small vitrified water droplets that were dome shaped and had

a contact angle of 90° (as seen for unmodified hydrophilic Pt/Al₂O₃), but there was no evidence of a vitrified layer over any parts of the surface to suggest strong local hydrophilicity. Instead, much of the water mist had formed spherical droplets with large contact angles (as seen for the silanated hydrophobic Pt/Al₂O₃) or had seeded into repeat layers of nano-crystals of ice, which were similar in size and morphology to the SiC crystallites.

Figure 2b shows the effect of including ceria in the formulation of a series of Pt/SiC catalysts, in which the Pt loading was 2, 1 or 0.5% by mass. To ensure maximum contact between the Pt and CeO₂, the support was first impregnated with cerium(IV) nitrate solution, and dried and calcined before impregnating with the platinum precursor. The effect of adding 1% ceria by mass was to suppress the activity of the catalysts, irrespective of Pt loading. However, the phenol conversion started to rise after it had reached a minimum at 1-2% loading of ceria. This inversion in activity is similar to the effects observed by Espinosa de los Monteros *et al* for either Pt or Ru supported on TiO₂-CeO₂.¹⁴ In the case of the catalyst with a 1% loading of platinum, after addition of 5% ceria its activity was comparable to that of the catalyst with a 2% loading of platinum dispersed on ceria-free SiC.

The same dependence of catalytic activity on support wettability was not reproduced when platinum was substituted by an equivalent loading of ruthenium (i.e. 2% by mass). Notably, in a comparison of catalytic performance at 140 °C for a series of ruthenium catalysts (Figure 3), ruthenium supported on the hydrophobic SiC had the lowest activity, which could not be improved by addition of ceria. However, the activity could be doubled by supporting the ruthenium on γ -Al₂O₃, and then doubled again by adding 5% ceria. The beneficial effect of ceria addition can also be seen in Figure 4, which shows a substantial difference in activity between 2%Ru-5%CeO₂ supported on alumina and 2%Ru-5%CeO₂ supported on silicon carbide, when measured as a function of temperature over the range 120-160 °C. This was reflected in the apparent activation energies, with the value for the alumina supported catalyst (21 kJ mol⁻¹) being less than half of that for the silicon carbide supported catalyst (47.5 kJ mol⁻¹).

Overall, our results clearly show that, in CWAO, there is a sensitivity between the activity of the precious metal and the nature of the underlying support material. In the case of platinum, starting with a benchmark Pt/Al₂O₃ catalyst, the activity could be increased in three ways, by (i) making the support hydrophobic (either through hydrophobation of the γ -Al₂O₃ or by replacing it with SiC), (ii) increasing the proportion of metal at the surface (by calcination in

nitrogen), and (iii) addition of ceria at a loading above a threshold of $\approx 2\%$ by mass. For ruthenium, however, optimum activity was achieved through the combination of a hydrophilic support and the inclusion of ceria (again $>2\%$ loading). The textural properties of our platinum and ruthenium catalysts were very consistent for each support, as expected for catalysts prepared from the same precursor and using the same preparation route. The most apparent difference between comparable pairs of catalysts was that the platinum was predominantly in its metallic form (Pt^0) whereas the ruthenium was present as RuO_2 .

The promoting effect of a water-repellent support (fluorinated carbon) on platinum was first demonstrated in the related field of vapour-phase oxidation, where the resultant catalyst could be used for the complete oxidation of methanol, formic acid and BTX contaminants even at temperatures below $100\text{ }^\circ\text{C}$.²³ A similar approach has since been used for CWAO in the work of Lavelle and McMonagle²⁴, who oxidised formic acid at near-ambient temperature in a spinning-basket reactor using platinum supported on a highly porous polydivinylbenzene support. They proposed that the presence of the hydrophobic support allowed a gas envelope to form around the active sites as the reactor rotated, which enhanced mass transfer of oxygen from the air feed to the catalyst surface, so minimising the limiting contribution of O_2 solubility in the condensed aqueous phase.²⁴ The inference from both these studies was that the optimum support material should always be hydrophobic in nature, irrespective of the identity of the active sites. By contrast, our results indicate that the optimum support is in fact active-site dependent, leading us to conclude that the different metal-support synergies that we observe reflect two different pathways for CWAO, in which the transport of O_2 from the air-feed to the active sites is the defining feature. We propose that, when ruthenium is used, RuO_2 adsorbs both reactants from the aqueous phase, and so a promoted hydrophilic support can be effective. When platinum is used, however, the Pt^0 active sites can adsorb phenol from the aqueous phase and O_2 directly from the gas phase, and therefore a largely hydrophobic support with highly localised hydrophilicity at or around the active sites is more effective. We suggest that the gas envelope (invoked by Lavelle and McMonagle²⁴), is more likely to exist as gas bubbles within the pore structures of our hydrophobic Pt catalysts when operating within a trickle-bed reactor. The secondary promoting effect of ceria on both Pt/SiC and $\text{Ru}/\text{Al}_2\text{O}_3$ is more difficult to rationalise. In previous CWAO studies, its intended function has been to increase the oxygen storage capacity of the catalyst,^{11,13,14} however its ability to store and transfer surface oxide ions is unlikely to play a part at the low temperatures used in our studies. Similarly, the promoting effect is unlikely to arise from a strong electronic metal-support interaction, as this

requires strongly reducing conditions either during preparation or use of the catalyst, but it may be indicative of the formation of a solid solution at the interface between the precious metal and the ceria.²⁵ This solid solution (which may account for the increased Lewis acidity reported in a previous study¹⁴) would confer hydrophilicity and additional phenol-adsorption sites at the metal-support interface, enabling a higher rate of phenol mass-transfer from the liquid phase to the Pt or Ru surface.

Supporting Information

Preparation and silanation of catalytic materials; diagram of trickle-bed reactor system and details of its use for catalyst testing; development of test methodology; additional characterisation of catalytic materials.

Acknowledgements

We gratefully acknowledge the financial support of Johnson Matthey and Cardiff University for this research, which was part of the Johnson Matthey *Bauhaus* programme.

References

1. Zimmermann, F. J. (Sterling Drug Inc.), Waste Disposal. *US Patent 2665249*, **1954**
2. Busca, G.; Berardinelli, S.; Resini, C.; Arrighi, L., Technologies for the removal of phenol from fluid streams: A short review of recent developments. *J. Hazard. Mater.*, **2008**, 160, 265-288
3. Bhargava, S. K.; Tardio, J.; Prasad J.; Foger, K.; Akolekar, D. B.; Grocott, S. C., Wet oxidation and catalytic wet oxidation. *Ind. Eng. Chem. Res.*, **2006**, 45, 1221-1258
4. Kolaczowski, S. T.; Plucinski, P.; Beltran, F. J.; Rivas, F. J.; McLurgh, D. B., Wet air oxidation: a review of process technologies and aspects in reactor design. *Chem. Eng. J.* **1999**, 73, 143-160
5. Tromans, D., Temperature and pressure dependent solubility of oxygen in water: a thermodynamic analysis. *Hydrometallurgy*, **1998**, 48, 327-342
6. Arena, F.; Di Chio, R.; Gumina B.; Spadaro, L.; Trunfio, G., Recent advances on wet air oxidation catalysts for treatment of industrial wastewaters. *Inorg. Chim. Acta*, **2015**, 431, 101-109

7. Wang, J.; Fu, W.; He, X.; Yang, S.; Zhu, W., Catalytic wet air oxidation of phenol with functionalized carbon materials as catalysts: Reaction mechanism and pathway. *J. Environ. Sci.*, **2014**, 26, 1741-1749
8. Guo, J.; Al-Dahhan, M., Kinetics of wet air oxidation of phenol over a novel catalyst. *Ind. Eng. Chem. Res.*, **2003**, 42, 5473-5481
9. Yang, S.; Cui, Y.; Sun, Y.; Yang, H., Graphene oxide as an effective catalyst for wet air oxidation of phenol. *J. Hazardous Materials*, **2014**, 280, 55-62
10. Kim, K.-H.; Ihm, S.-K., Heterogeneous catalytic wet air oxidation of refractory organic pollutants in industrial wastewaters: a review. *J. Hazardous Materials*, **2011**, 186, 16-34
11. Oliviero, L.; Barbier Jr., J.; Duprez, D.; Wahyu, H.; Ponton, J. W.; Metcalfe, I. S.; Mantzavinos, D., Wet air oxidation of aqueous solutions of maleic acid over Ru/CeO₂ catalysts. *Appl. Catal. B: Environ.*, **2001**, 35, 1-12
12. Cybulski, A.; Trawczynski, J., Catalytic wet air oxidation of phenol over platinum and ruthenium catalysts. *Appl. Catal. B: Environ.*, **2004**, 47, 1-13
13. Barbier Jr., J.; Oliviero, L.; Renard, B.; Duprez, D., Role of ceria-supported noble metal catalysts (Ru, Pd, Pt) in wet air oxidation of nitrogen and oxygen containing compounds. *Topics in Catalysis*, **2005**, 33, 77-86
14. Espinosa de los Monteros, A.; Lafaye, G.; Cervantes, A.; Del Angel, G.; Barbier, Jr., J.; Torres, G., Catalytic wet air oxidation of phenol over metal catalyst (Ru,Pt) supported on TiO₂-CeO₂ oxides. *Catal. Today*, **2015**, 258, 564-569
15. Lunagómez Rocha, M.A.; Del Ángela, G.; Torres-Torres, G.; Cervantes, A.; Vázquez A.; Arrieta, A.; Beltramini, J.N., Effect of the Pt oxidation state and Ce³⁺/Ce⁴⁺ ratio on the Pt/TiO₂-CeO₂ catalysts in the phenol degradation by catalytic wet air oxidation (CWAO). *Catal. Today*, **2015**, 250, 145-154
16. Yuan, Y.; Lee T. R., Contact angle and wetting properties. In *Surface Science Techniques*, Bracco, G., Holst, B., Eds.; Springer, **2013**; pp. 3-34
17. Guichard, P.; Hamel, V.; Le Guennec, M.; Banterle, N.; Iacovache, I.; Nemcikova, V.; Fluckiger, I.; Goldie, K.N.; Stahlberg, H.; Levy, D.; Zuber, B.; Gonczy, P., Cell-free reconstitution reveals centriole cartwheel assembly mechanisms. *Nature Comm.*, **2017**, 8:14813
18. Ditscherlein, L.; Fritzsche, J.; Peuker, U. A., Study of nanobubbles on hydrophilic and hydrophobic alumina surfaces. *Colloids and Surfaces A: Physicochem. Eng. Aspects*, **2016**, 497, 242-250

19. Sah, A.; Castricum, H. L.; Blik, A.; Blank, D. H. A.; ten Elshof, J. E., Hydrophobic modification of γ -alumina membranes with organochlorosilanes. *J. Membrane Sci.*, **2004**, 243, 125-132
20. U.S. EPA (Environmental Protection Agency), Hazardous waste management system; identification and listing of hazardous waste; solvents; final rule. *Federal Register 63 FR*, **1998**, pp. 64371-64402
21. Martín-Hernández, M.; Carrera, J.; Suárez-Ojeda, M. E.; Besson, M.; Descorne, C., Catalytic wet air oxidation of a high strength p-nitrophenol wastewater over Ru and Pt catalysts: Influence of the reaction conditions on biodegradability enhancement. *Appl. Catal. B: Environ.*, **2012**, 123-124, 141-150
22. Medout-Marere, V.; El Ghzaoui, A.; Charnay, C.; Douillard, J. M.; Chauveteau, G.; Partyka, S., Surface heterogeneity of passively oxidized silicon carbide particles: Hydrophobic–hydrophilic partition. *J. Colloid and Interface Science*, **2000**, 223, 205-214
23. Chuang, K. T.; Zhou, B., Tong, S., Kinetics and mechanism of catalytic oxidation of formaldehyde over hydrophobic catalysts. *Ind. Eng. Chem. Res.*, **1994**, 33, 1680-1686
24. Lavalle, K.; McMonagle J. B., Mass transfer effects in the oxidation of aqueous organic compounds over a hydrophobic solid catalyst. *Chem. Eng. Sci.*, **2001**, 56, 5091-5102
25. Acerbi, N.; Golunski, S.; Tsang, S. C.; Daly, H.; Hardacre, C.; Smith, R.; Collier, P., Promotion of ceria catalysts by precious metals: Changes in nature of the interaction under reducing and oxidizing conditions. *J. Phys. Chem. C*, **2012**, 116, 13569-13583

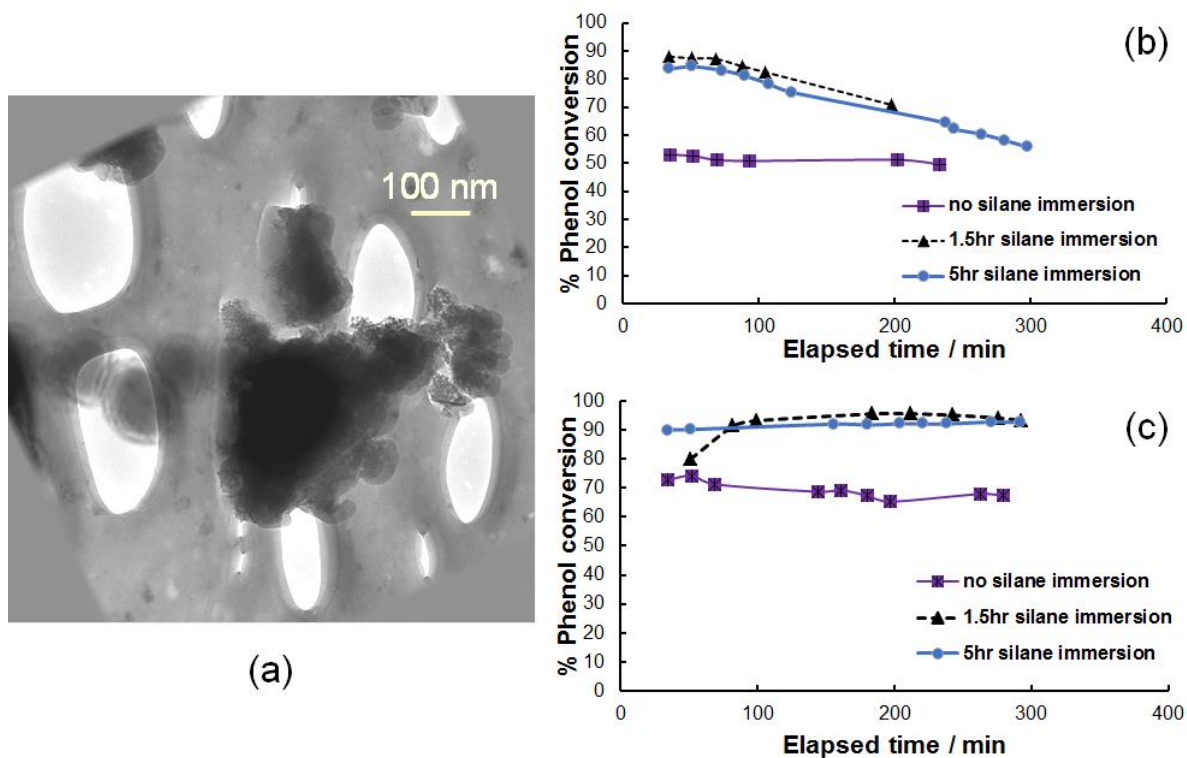


FIGURE 1: (a) Single CEM image of unsilanated Pt/Al₂O₃; (b) performance at 140 °C of unsilanated and silanated Pt/Al₂O₃; (c) performance at 120 °C of unsilanated and silanated Pt/Al₂O₃ following additional calcination under N₂. (Test conditions: P = 13.1 bar_g; liquid feed concentration = 1000 mg litre⁻¹ phenol in water; LHSV = 26.6 h⁻¹; air feed rate = 144 cm³ min⁻¹; trickle-bed reactor.)

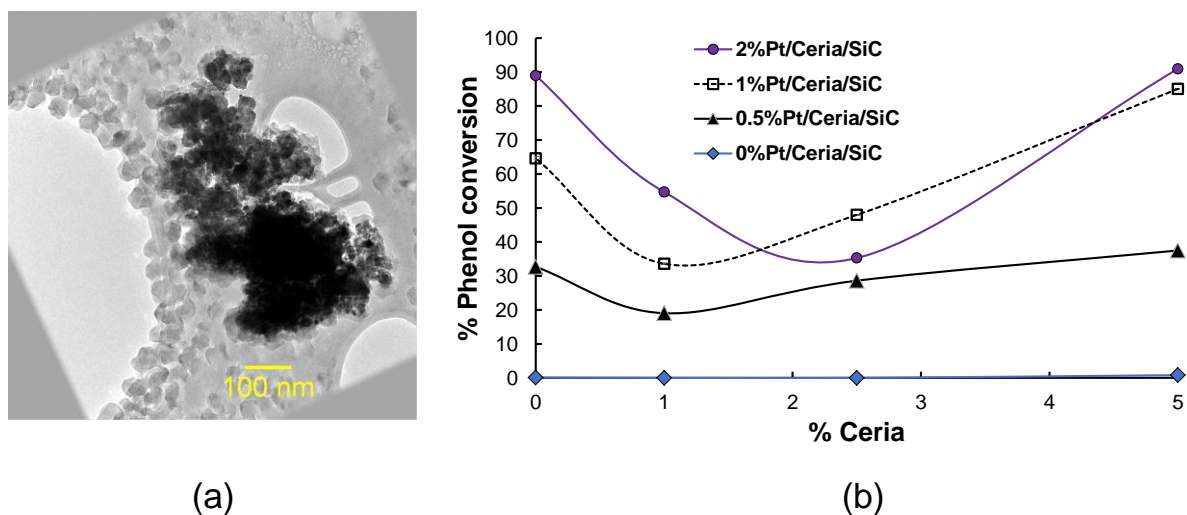


FIGURE 2: (a) Single CEM image of Pt/SiC; (b) Effect on performance at 120 °C of ceria addition to Pt/SiC catalysts with varying Pt loadings. (Test conditions as in Figure 1.)

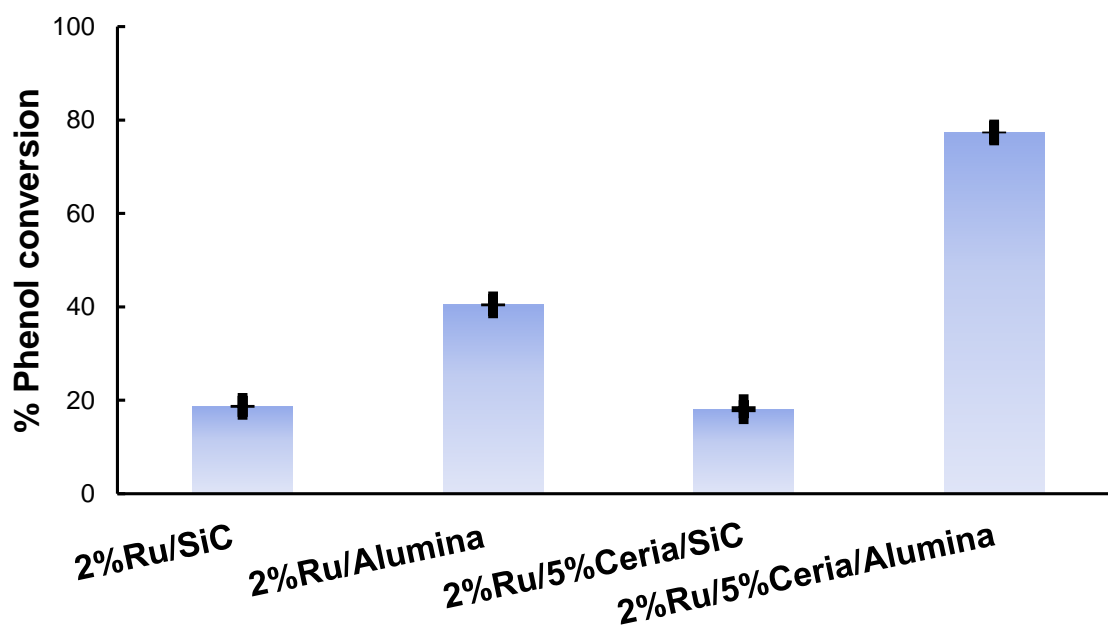


FIGURE 3: Comparative performance of Ru catalysts at 140 °C, with error bars indicated for the conversion measurements at steady state. (Test conditions as in Figure 1.)

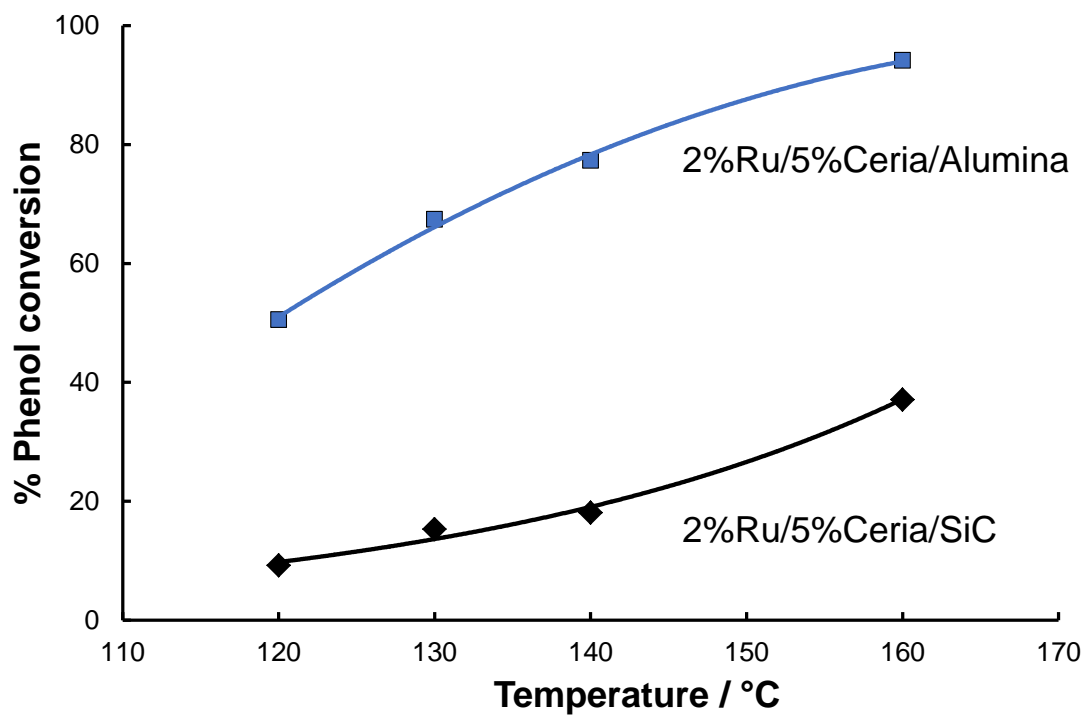


FIGURE 4: Comparative performance of hydrophobic (2% Ru/5% Ceria/SiC) and hydrophilic (2% Ru/5% Ceria/Alumina) Ru catalysts as function of temperature. (Test conditions as in Figure 1.)